Journal of Education and Science (ISSN 1812-125X)

# Synthesis, Characterization and Study of the Antibacterial Activity of $CuFe_2O_4$ Nanoparticles and Their Toxicity Measurement

**E. M. Esmail [(1)], M. S. Ghafouri [(2)], N. A. Hasan [(3)], A. M. Rashed [(4)*]**

[(1,2)] The General Directorate for Education of Diyala, Diyala, Iraq
[(3,4)] Department of Chemistry, College of Education for Pure Science, University of Diyala, Iraq

**Article information**

***Article history:***
Received: November 07, 2025
Revised: March 17, 2026
Accepted: March 25, 2026
Available online: July 01, 2026

***Keywords***:
$CuFe_2O_4$ Nanoparticles
HUVECs
E. Coli
Cytotoxicity

***Correspondence:***
***Athraa Mohamed Rashed***
atharymoh1996@gmail.com

**Abstract**

Metallic nanoparticles (NPs) have enormous applications due to their remarkable physical and chemical properties. The synthesis of NPs has been a matter of concern because chemical methods are toxic. $CuFe_2O_4$ spinel nanocomposites were prepared using green chemistry method and characterized using Fourier transform infrared (FTIR), scanning electron microscopy (SEM), EDX spectroscopy, and X-ray diffraction (XRD). The FTIR spectroscopy of $CuFe_2O_4$ showed two broad bands at 365 and 547 $cm^{-1}$. The X-ray diffraction results showed that the average particle size was 30.62 nm. The scanning electron microscope (SEM) images exhibited an irregular dislike morphology of nanoparticles that agglomerated more in the case of green synthesis. The SEM micrograph of $CuFe_2O_4$ nanoparticles with a predominantly spherical shape. The particles exhibit significant agglomeration, resulting in an average diameter of approximately 107.24 nm. The inhibition of the prepared $CuFe_2O_4$ composites on *Escherichia coli* bacteria isolated from Diyala River water was studied. The inhibition of the spinel nanocomposites was measured using five successive concentrations (500, 600, 700, 800, 900, and 1000) µg/ml. The results showed that $CuFe_2O_4$ exhibited growth inhibitory activity against E. coli, with the highest growth inhibition rate against. At 1000 µg/ml, the *E. coli* concentration was 63.2%. At 500 µg/ml, the lowest growth inhibition rate against *E. coli* was 17.6%. The toxicity of $CuFe_2O_4$ compounds was studied on the HUVEC endothelial cell line. An MTT assay was performed using a device. The survival rate of HUVEC cells after 48 hours of adding copper ferrite ($CuFe_2O_4$) at a concentration of (25µg/ml) was 99.70%, which is the lowest concentration, while at the highest concentration (400µg/ml), the survival rate of HUVEC cells was 45.38%, and the value was (IC50=311).

DOI:10.33899/jes.v35i3.53784, 

## 1. Introduction

Nanotechnology has become one of the most interesting areas of scientific research in the past few years. It is receiving much attention in material research, including synthesis, characterization and applications of nanometer-sized metals, oxides, semiconductors and ceramics [1]. Nanomaterials have many applications in areas ranging such as catalysis, photonics, molecular computing, energy storage, fuel cells, tunable resonant devices, sensing to nano medicine [2]. This is due to an increase in reactivity when compared to their micro-sized counterparts since nano-scaled materials exhibit a larger surface to- volume ratio, which provides unsaturated and thus, more reactive surface atoms. NPs nanoparticles are primary particles with a diameter smaller than 100 nm. The most common NPs have been made from transition metals, silicon, carbon, and metal oxides. The research of metal oxide has been intense scientific interest due to a wide variety of potential applications in biomedical, optical and electronic fields. it can be produced through either chemical or physical means [3, 4].$CuFe_2O_4$ NPs are the fascinating

versatile material and highly outstanding due to its intrinsic magnetic properties ,It is extensively used for a variety of applications such as microwave; electronic devices from low to high permeability including ferrofluids, loading coil, microwave devices, magnetic drug delivery, gas sensor, color imaging, antenna rod, recording head, and high-density information storage; LPG gas sensing; and photocatalytic applications[5] and Its application is further extended to biomedicine and drug delivery, magnetic resonance imaging, magnetic separation of cancer cells and antibacterial activities[6]. The most common and known formula for a spinel ferrite is reported by several works, $MFe_2O_4$ (M = $Ni^{2+}$, $Cu^{2+}$, $Co^{2+}$, $Zn^{2+}$, and$Mn^{2+}$) or $M^{2+}Fe^{3+}{}_2\ O^{2-}{}_4$ where divalent and trivalent cations correspond to $M^{2+}$ and $Fe^{3+}$, respectively [7]. Copper ferrite is formed in two crystal structures namely cubic spinel and tetragonal phases depending upon the method of preparation and annealing temperature. General preparative methods of copper ferrite include hydrothermal method, sono-chemical method, citrate-nitrate, sol-gel method, co-precipitation method, solid-state method and green synthesis methods.[8-10]

## 2. Materials and Methods

All materials were analytical grade and used as purchased without further purification. $Cu(NO_3)_2.6H_2O$, $Fe(NO_3)_3.9H_2O$, anhydrous citric acid, $NH_4OH$, and deionized water were purchased from Sigma-Aldrich. Water samples were collected from specific sites along the Diyala River using sterile glass bottles. The isolation of Escherichia coli was carried out using the membrane filtration method (or the direct plate count method). Portions of the water samples were inoculated onto MacConkey agar and incubated at 37°C for 24 hours. To confirm the identity of E. coli, characteristic pink colonies were streaked onto Eosin Methylene Blue (EMB) agar, where they exhibited a distinctive metallic green sheen. The isolates were further validated through Gram staining, showing Gram-negative rods, and standard biochemical IMViC tests to ensure the accuracy of the environmental isolates used in this study.

### 2.1. Synthesis and characterization

#### 2.1.1. Preparation of $CuFe_2O_4$ nanoparticles

Preparation of $CuFe_2O_4$ by green chemistry .Mix 1.5 g of $Cu(NO_3)_2.6H_2O$,1.5g of $Fe(NO_3)_3.9H_2O$, and 1.5 g of Anhydrous Citric acid in 150 ml of ionic water and put on the magnetic stirrer at 25 $C^0$ for 20 min. The pH was adjusted to 7.5 by adding 25% $NH_4OH$. The mixture at 135 $C^0$ until the formation of a gel and the formation of a precipitate.

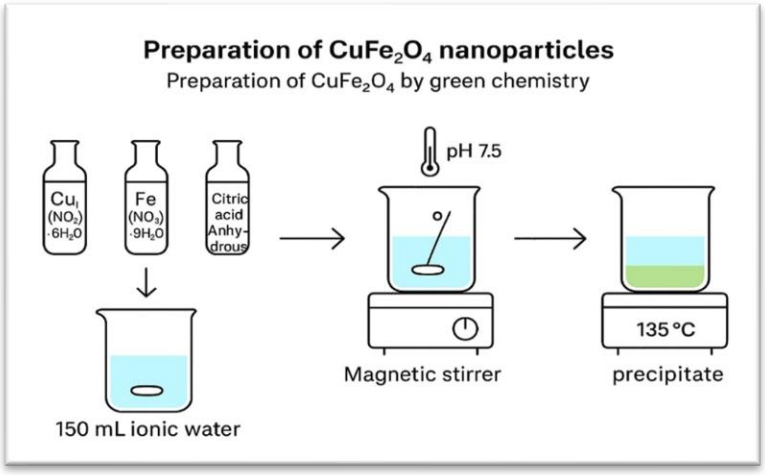


**Figure 1**: Steps for synthesizing nano copper ferrite.

#### 2.2.2. Characterization techniques

The University of Tehran, Iran's College of Science conducted all of the sample analysis. The XRD pattern was obtained using a Siemens model D500 by irradiating the samples with 40 kV at scanning angles ranging from 20$C^0$ to 80$C^0$.Using a Shimadzu (Tokyo, Japan) FTIR spectrophotometer and KBr pellet, the materials' FTIR spectra were acquired. A Zeiss SEM (Germany) operating at 200 kV was used for the SEM analysis.

#### 2.2.3. Antibacterial activity (Broth microdilution method)

To evaluate the antibacterial potential, 1.5 (mg)of $CuFe_2O_4$ NPs were suspended in 1.5 (ml) of sterile deionized water to prepare a stock solution. The suspension was subjected to ultrasonication for 35 (minutes) with 5 (minute) intervals using a water bath sonicator, followed by vigorous vortexing and storage at 4ºC to maintain stability. A series of dilutions for $CuFe_2O_4$ NPs (500–1000 µg/ml) were prepared in sterile 96-well microtiter plates. This range was selected based on preliminary screening and previously reported MIC values for ferrite nanoparticles [11]. The bacterial isolates of Escherichia coli used in this study were locally isolated from water samples collected from the Diyala River, Iraq. For identification, the samples were cultured on selective and differential media, including MacConkey agar and Eosin Methylene Blue (EMB) agar. The isolates were further confirmed using standard biochemical tests (IMViC tests) and validated by the VITEK. The bacterial inoculum of *Escherichia coli* (ATCC 25922) was adjusted in Mueller-Hinton Broth to match the 0.5 McFarland standard (108 CFU/ml). Each well, containing 100 µl/well of NPs or amoxicillin (as a standard antibiotic), was inoculated with 100 µl/well of the bacterial suspension. Three wells containing only the bacterial inoculum and medium served as the Positive Control (Growth Control), while three wells with only the medium served as the Negative Control (Blank). After incubation at 37 Cº for 24 hours, the optical density was measured at 630 nm using a Biotech Synergy HT Multimode Microplate Reader. The Growth Inhibition percentage (GI%) was calculated using the following equation [12]:

$$\mathbf{GI\% = (OD_{630\ of\ antibacterial\ agent} - OD_{630\ of\ positive\ control})/OD_{630\ of\ positive\ control} \times 100.}$$

Where:

• Positive Control: Medium + Bacteria.

• Antibacterial Agent: Medium + Bacteria + CuFe_2O_4 NPs.

### 2.2.4. MTT assay for $CuFe_2O_4$ nanoparticles

MTT 3-[4,5-dimethylthiazole-2-yl]-2,5-diphenyltetrazolium bromide dye (10 mg/ml) were used in this test. After dissolving the $CuFe_2O_4$ nanoparticle sample in 0.2% DMSO, a gradient concentration of 25, 50, 100, 200, and 400 µg/ml was obtained. A 200 µl aliquot of suspended cells ($1\times10^4$ cells/well) made in RPMI media was seeded into 96 well microplate and incubated for 24 hours at 37 °C with 5% $CO_2$. Twenty microlitres of $CuFe_2O_4$-NPs were added to the cell cultures, and they were then incubated for twenty-four hours under the same conditions. Each sample was then mixed with 10 µl of MTT reagent and incubated for five hours at 37°C. At 570 nm, the absorbance was measured. utilizing an ELISAREADER (DANA-3200). This assay employed two controls: control-1, which included cells treated with DMSO, and control-2, which included only untreated cells. Both the IC50 and the inhibition percentage were computed and statistically examined [13].

### 2.2.5. Statistical analysis

GraphPad Prism 9 (GraphPad Software, La Jolla, CA, USA) was used to perform statistical analyses. Tukey's multiple comparisons test and one-way ANOVA were employed to compare the tested groups. The findings are shown as mean ± SD, and a significance level of $p<0.05$ was applied.

## 3. RESULTS AND DISCUSSION

### 3.1. Morphological analysis for $CuFe_2O_4$-NPs

The process of co-precipitation was used to create $CuFe_2O_4$-NPs. X-ray diffraction was used to characterize the produced nanoparticles' crystal structure and phase purity, as illustrated in Fig 2. The International Centre for X-ray diffraction (ICDD) card number (34-0425) data and the X-ray diffraction spectrum of the synthesized spinel iron ($CuFe_2O_4$) were compared [8]. The spinel iron nanoparticle's average crystal size was determined. It was 30.62 nm using the (Debye-Scherer) equation.1[14]

$$D = \frac{K\lambda}{\beta cos\theta} \text{.....1}$$

D = average crystal size (nm)

K = constant that depends on the crystal form (0.94 -0.89)

**λ** = X-ray wavelength (1.54059 Å) (most λ for copper)

B = FWHM mid-highest peak

θ= Prague angle.

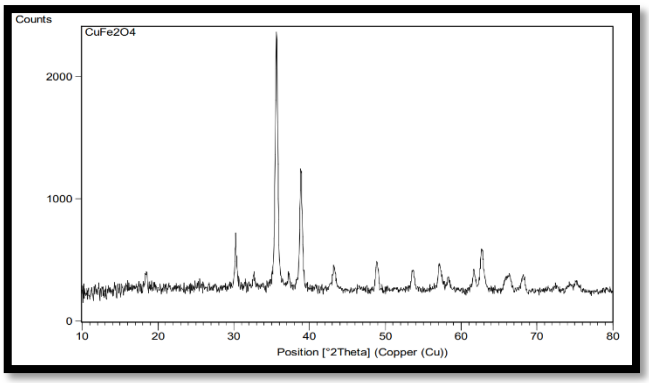


### 3.2. FTIR study for $CuFe_2O_4$-NPs

The copper ferrite ($CuFe_2O_4$) ferrite was identified by tracing its infrared (FT-IR) spectrum and comparing it with the spectrum of Cu $(NO_3)_2.6H_2O$ and Fe $(NO_3)_3.9H_2O$ salts as shown in Figure 3. The appearance of a sharp and medium beam at the frequency (365 $cm^{-1}$) refers to the stretching of the U (Cu-O) band, and another sharp and long band at frequency (546 $cm^{-1}$) is due to the stretching of the U (Fe-O) band. It was also observed that a sharp and long band at frequency (1384 $cm^{-1}$) belongs to the (C-O) band stretching, and a wide and medium band at the frequency (1616 $cm^{-1}$) cm belongs to the U band stretching (C = O). And the emergence of a wide and distinct band at the frequency (3448 $cm^{-1}$) due to the stretching of the U (O-H) band.[15, 16]

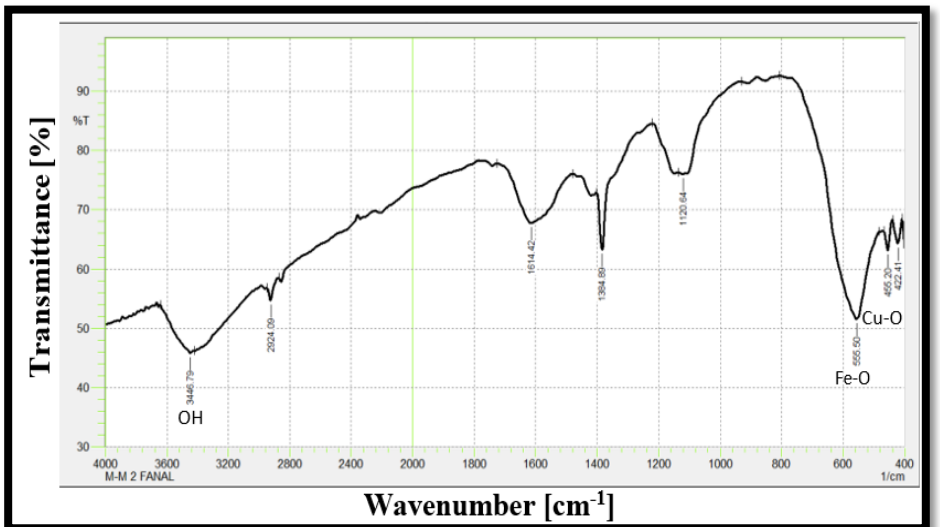


**Fig.3** The infrared spectrum of $CuFe_2O_4$ nanoparticles

### 3.3. SEM analysis for $CuFe_2O_4$-NPs

Using scanning electron microscopy (SEM), the morphological and structural makeup of copper ferrite nanoparticles ($CuFe_2O_4$) were investigated. as seen in Figure 4, and the SEM images the copper ferrite nanoparticles are within the nanometer range, revealed that while the majority of the nanoparticles were present in the form of clustering, some were widely separated from one another. Electrostatic forces are responsible for this agglomeration, which is in line with comparable behavior to nanoparticle agglomeration observed in earlier research. These nanoparticles have an average diameter of roughly 107.24 nm [17]

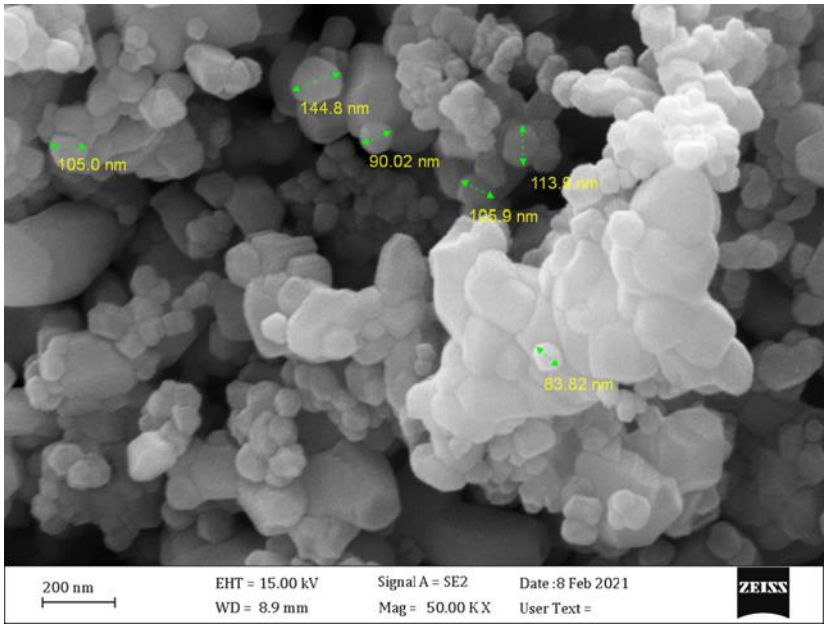


**Fig.4 An SEM image of $CuFe_2O_4$ nanoparticles**

### 3.4. Energy Dispersive X-ray (EDX) for $CuFe_2O_4$-NPs.

The proportion of elements present in the nanocrystalline copper ($CuFe_2O_4$) ferrite was determined by energy-dispersive X-ray EDX. As shown in Figure 5, the results showed the presence of copper (55.8%) and iron (22.3%). The presence of very small proportions of each of the element oxygen, molybdenum, carbon, calcium and the prepared spinel of good purity.[18, 19]

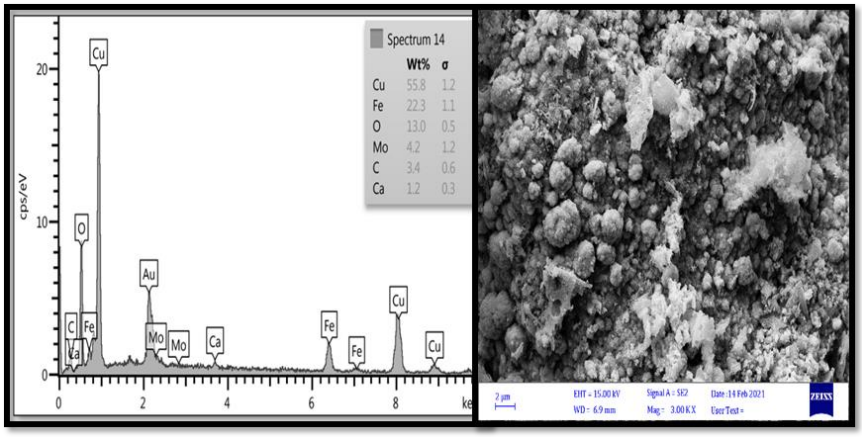


**Fig.5 An EDX image of $CuFe_2O_4$ nanoparticles.**

### 3.5. Atomic force microscopy (AFM) for $CuFe_2O_4$-NPs.

The as-prepared copper ($CuFe_2O_4$) ferrite was analyzed using atomic force microscopy (AFM) and the size ratio of the particles was Ave. Diameter) was (66.4 nm), the mean roughness was (122pm) and the (Sq. Root mean square) was (250pm) picometers as shown in Figure 6 [20].

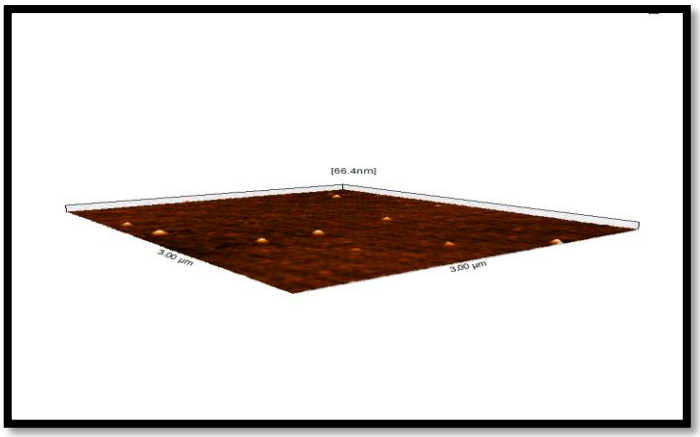


**Fig.6** Atomic force microscopy (AFM) image of Nano copper spinel ferrite ($CuFe_2O_4$)

### 3.6. Antibacterial activity for $CuFe_2O_4$ -NPs.

The effect of adding different concentrations of nano-copper ferrite ($CuFe_2O_4$) on inhibiting the growth of *E. coli* bacteria was studied as shown in Table (1) and Figure 7. the results demonstrated a clear direct correlation between $CuFe_2O_4$ concentration and the rate of bacterial inhibition. The direct correlation between the increased concentration of $CuFe_2O_4$-NPs and the bacterial inhibition can be attributed to two main mechanisms. First, higher concentrations of nanoparticles enhance the production of Reactive Oxygen Species (ROS), which leads to significant damage to the bacterial cell walls. Second, the Cu and Fe molecules possess the ability to penetrate the outer membrane of Gram-negative *E. coli*, further disrupting cellular functions and inhibiting growth. When 1000 µg/ml of *E. coli* is present, the rate of growth inhibition is 63.2%. The lowest percentage of growth inhibition towards *E. coli* was 19.6% at a concentration of (500 µg/ml). The results of statistical analysis showed copper ferrite ($CuFe_2O_4$) on the growth inhibition of *E. coli* bacteria using (Graph Pad Prism 9) program, and (correlation) analysis was used to infer the significance The value was (P-value <0.0002) and there is a significant difference between the concentration and the percentage of survival of cells, Significant diff. Among means ($P < 0.05$) and the value of R square was (0.9682), which indicates a strong correlation between the inhibition of the growth of Escherichia coli bacteria and the increase in the concentration of ($CuFe_2O_4$) [10, 21, 22].

**Table (1).Effect of $CuFe_2O_4$ concentration on bacterial growth inhibition (%)**

| **Compound** | **Inhibition (%) Mean±SD standard deviation Concentration (µg/ml)** | | | | | |
|---|---|---|---|---|---|---|
| | **500** | **600** | **700** | **800** | **900** | **1000** |
| $CuFe_2O_4$ | 19.6±0.76 | 27.1±0.16 | 30.4±3.77 | 40.1±2.37 | 50.5±1.94 | 63.2±0.69 |

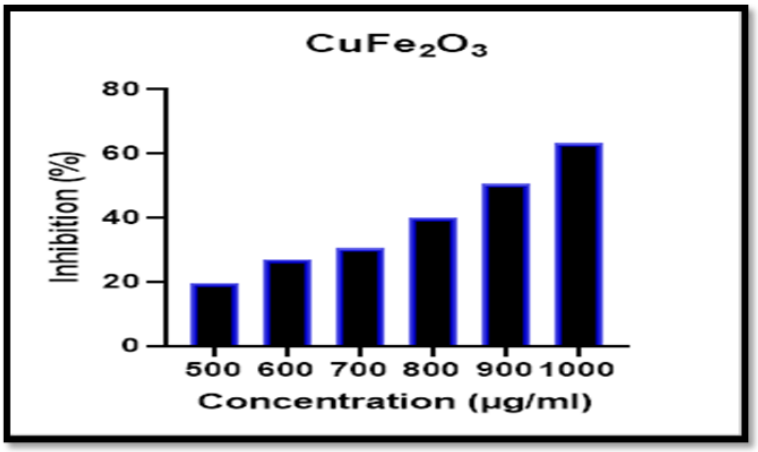


**Fig.7** The effect of nanocrystalline copper ferrite concentration on the growth inhibition of *E. coli*

The antibacterial activity of micronutrients was studied using *E. coli bacterium*, as prepared nanocrystalline copper ferrite ($CuFe_2O_4$) showed many advantages which are the performance of targeted biomolecules such as stability, monodispersion, simplicity, low cost and fast separation. On the other hand, the results showed that it has an effective antibacterial effect against. *E. coli bacteria* and has the ability to reduce functional proteins on the bacterial cell membrane ($CuFe_2O_4$) was also widely used in water treatment, and it meets the safety standards of public drinking water. The results indicated that the ROS content is high inside the cell, which may impair vital cellular components and cause extravasation, presumably to be the cause of E. coli cell death. As shown in Figure 8, the control plates exhibited dense bacterial growth on nutrient agar (Figure 8A) and MacConkey agar (Figure 8C). In contrast, treatment with the nano-spinel $CuFe_2O_4$ compound resulted in a marked decrease in bacterial growth on nutrient agar (Figure 8B) and a significant reduction in the number of colonies on MacConkey agar (Figure 8D), demonstrating the antibacterial activity of the nano-spinel compound. [23]

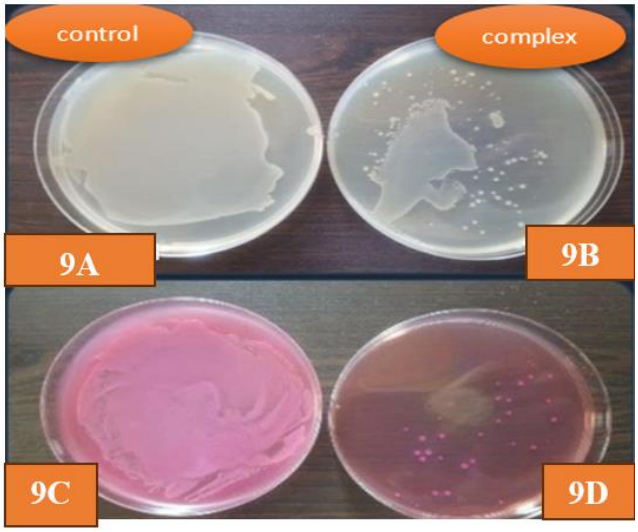


**Fig.8 Antibiotic test of nanocomposites against E. coli bacteria.**

### 3.7. Toxicity test of nano copper ferrite ($CuFe_2O_4$) on HUVEC cells

The results shown in Table 2 showed the cytotoxicity and were investigated at varying concentrations (ranging from 25 to 400 µg/ml). Compared to the control group, the results showed that the percentage of HUVEC cell survival after 48 hours of adding copper ferrite ($CuFe_2O_4$) at a concentration of (25 µg/ml) was 99.70%, indicating that there is a relationship between the time factor and concentration on the percentage of HUVEC cell survival. However, we find that the percentage of HUVEC cell survival at a 50 µg/ml concentration was 88.44%. The percentage decreased, indicating that there is a relationship between increasing the concentration and the percentage of effectiveness or killing. While the percentage of cell survival at a concentration of (100 µg/ml) was 79.92%, as it appears that the percentage decreased. At a concentration of (200 µg/ml), the

percentage of HUVEC cell survival was 64.87%, as it appears that the percentage decreased to half, but at a concentration of (400 µg/ml), the percentage of HUVEC cell survival was 45.38%, indicating a decrease in the number of living cells by more than half, as shown in Table 2 and Figure 9.

**Table 2 shows the cytotoxicity of copper nano ferrite at 48 hours for HUVEC cells.**

| Concentration | R1% | R2% | R3% | Mean% | SD |
|---|---|---|---|---|---|
| 0 | 101.8288 | 98.83626 | 99.335 | 100 | 1.603266 |
| 25 | 101.0807 | 100.3325 | 97.71405 | 99.70906 | 1.767760 |
| 50 | 87.24023 | 87.73899 | 90.35744 | 88.44556 | 1.674418 |
| 100 | 79.38488 | 78.51206 | 81.87864 | 79.92519 | 1.74712 |
| 200 | 67.91355 | 62.55196 | 64.17291 | 64.87947 | 2.749746 |
| 400 | 43.10059 | 47.2153 | 45.84373 | 45.38654 | 2.095109 |

While the results of the statistical analysis showed that the nano-copper ferrite ($CuFe_2O_4$) on HUVEC cells in 48 hours reached a value of (P-value < 0.0003) and there is a significant difference between the concentration and the percentage of cell survival (Significant diff. Among means (P < 0.05) yes) and the value of R square was equal to (0.9599), which indicates the presence of a high degree of connection among the variables. The inhibitory concentration at half maximum (IC50) of nano-copper ferrite on HUVEC cells in 48 hours was measured using the program (Graph Pad Prism 9.0) using normalized response analysis and the value was (IC50= 311 µg/ml), as shown in Figure 10.

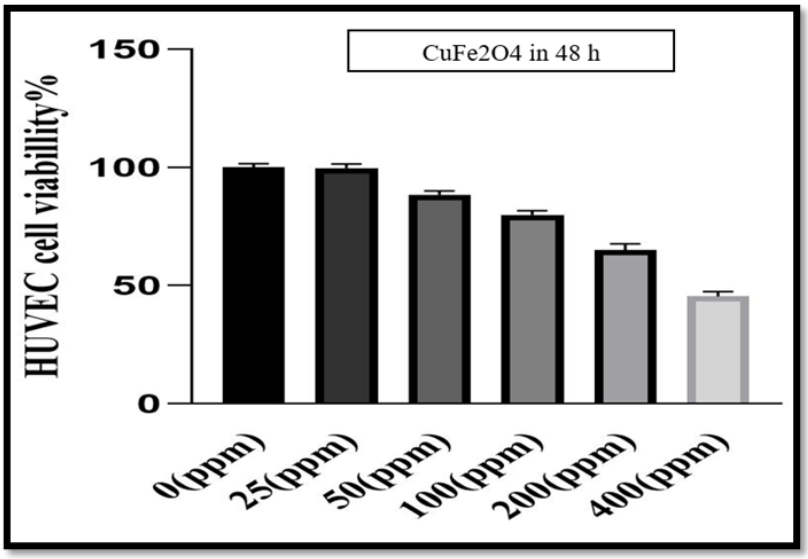


**Figure 9.**MTT assay of copper (CuFe2O4) nanoparticles on HUVEC at 48 hours

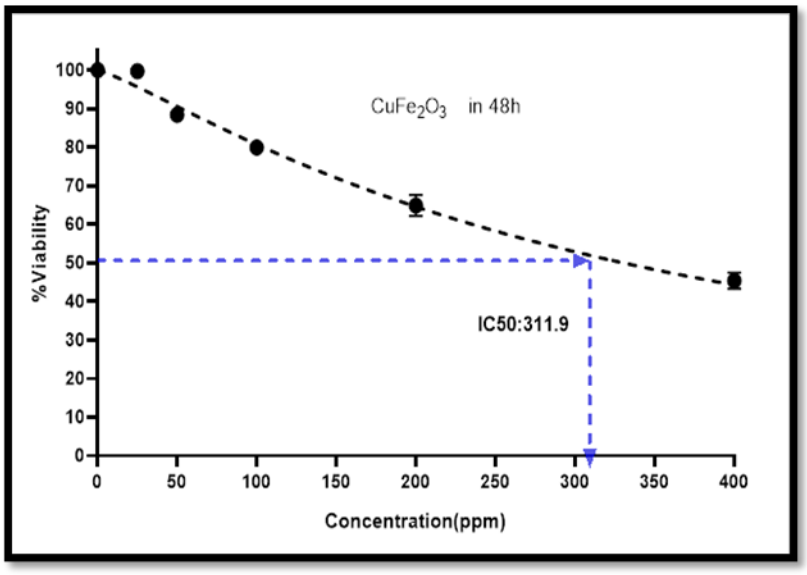


**Figure 10.** IC50 for nanocrystalline copper ferrite ($CuFe_2O_4$) at 48 hours

Copper ferrite ($CuFe_2O_4$) has gained significant interest because of its fascinating optical, electrical, and magnetic characteristics in recent years. When manufactured under different conditions, it exhibits electrical switching, phase transitions, and changes in semiconductor characteristics, making it one of the most significant spinel ferrites. It has remarkable chemical and thermal stability in addition to intriguing magnetic and electrical characteristics [16]. The goal of this study was to find out how cytotoxic $CuFe_2O_4$ NPs were to HUVEC cells.

Cell viability, cell membrane damage, cell cycle, mitochondrial membrane potential, and the expression of certain apoptotic genes in HUVEC cells were all assessed in order to accomplish this aim. We also investigated whether one of the potential mechanisms of cytotoxicity is the production of intracellular reactive oxygen species (ROS) as a result of exposure to $CuFe_2O_4$ NPs [20].

## 4. CONCLUSION

The structural properties of the CuFe2O4 nanoparticles were characterized using FTIR, XRD, and SEM. XRD and SEM examinations revealed that the average size of the CuFe2O4 nanoparticles was 30.62 nm in XRD and 107.24 nm in SEM. This study highlights the significant potential of green-synthesized $CuFe_2O_4$ nanoparticles as potent antibacterial agents, particularly against *E. coli* isolated from environmental water sources. The antibacterial efficacy was found to be concentration-dependent, achieving a maximum inhibition rate of 63.2%. Furthermore, cytotoxicity evaluations on HUVEC cells revealed that the nanocomposites maintain high biocompatibility at low concentrations, while exhibiting a clear dose-response relationship with an IC50 value of 311. Consequently, these nanoparticles represent a promising candidate for biomedical and water treatment applications.

## 5. Acknowledgments

The authors appreciate the College of Education for Pure Sciences - University of Diyala for using laboratories with the necessary equipment to carry out the experiment.

## 6. Conflicts of interest

The authors have confirmed that they have no personal stakes in the outcome of this work.

## 7. Funding

The authors have not received any financial support for implementation and publication this paper.

## 8. Conflicts of Interest

The authors declare that there are no conflicts of interest

## 9. REFERENCES


1. Stankic, S., et al., *Pure and multi metal oxide nanoparticles: synthesis, antibacterial and cytotoxic properties.* Journal of nanobiotechnology, 2016. **14**(1): p. 73. DOI:10.1186/s12951-016-0225-6
2. Bhuvaneshwari, B., S. Sasmal, and N.R. Iyer. *Nanoscience to nanotechnology for civil engineering: proof of concepts*. in *Proceedings of the 4th WSEAS International Conference on Recent Researches in Geography, Geology, Energy, Environment and Biomedicine (GEMESED'11)*. 2011. DOI:10.1186/s12951-016-0225-6
3. Baig, N., I. Kammakakam, and W. Falath, *Nanomaterials: A review of synthesis methods, properties, recent progress, and challenges.* Materials advances, 2021. **2**(6): p. 1821-1871 DOI: 10.1039/D0MA00807A.
4. Chandrakala, V., V. Aruna, and G. Angajala, *Review on metal nanoparticles as nanocarriers: Current challenges and perspectives in drug delivery systems.* Emergent Materials, 2022. **5**(6): p. 1593-1615. DOI: 10.1007/s42247-022-00404-5
5. Zaharieva, K., et al., *Preparation, characterization and application of nanosized copper ferrite photocatalysts for dye degradation under UV irradiation.* Materials Chemistry and Physics, 2015 :160 . p. 271-278. DOI: 10.1016/j.matchemphys.2015.03.018
6. Wang, H., et al., *Multifunctional PEG encapsulated Fe 3 O 4@ silver hybrid nanoparticles: antibacterial activity, cell imaging and combined photothermo/chemo-therapy.* Journal of Materials Chemistry B, 2013. **1**(45): p. 6225-6234. DOI: 10.1039/C3TB21052A
7. Masoumi, S., G. Nabiyouni, and D. Ghanbari, *Photo-degradation of azo dyes: photo catalyst and magnetic investigation of CuFe2O4–TiO2 nanoparticles and nanocomposites.* Journal of Materials Science: Materials in Electronics, 2016. **27**(9): p. 9962-9975DOI: 10.1007/s10854-016-5033-9.
8. Yang ,D., et al., *High-surface-area disperse silica nanoparticles prepared via sol-gel method using L-lysine catalyst and methanol/water co-solvent.* Colloids and Surfaces A: Physicochemical and Engineering Aspects, 2021. **610**: p. 125700. DOI: 10.1016/j.colsurfa.2020.125700
9. El Mouden, A., et al., *Removal of cadmium and lead ions from aqueous solutions by novel dolomite-quartz@ Fe3O4 nanocomposite fabricated as nanoadsorbent.* Environmental Research, 2023. **225**: p. 115606. DOI: 10.1016/j.envres.2023.115606
10. El Messaoudi, N., et al., *Green synthesis of CuFe2O4 nanoparticles from bioresource extracts and their applications in different areas: a review.* Biomass Conversion and Biorefinery, 2025. **15**(1): p. 99-120. DOI: 10.1007/s13399-023-04115-7
11. Azam, A., et al., *Antimicrobial activity of metal oxide nanoparticles against Gram-positive and Gram-negative bacteria: a comparative study.* International journal of nanomedicine, 2012: p. 6003-6009. DOI: 10.2147/IJN.S35347
12. WH, H.-A., N. Mohd-Al-Faisal, and A. Fathilah, *Determination of the percentage inhibition of diameter growth (PIDG) of Piper betle crude aqueous extract against oral Candida species.* Journal of Medicinal Plants Research, 2011. **5**(6): p. 878-884.
13. Dabagh, S., S.A. Haris, and Y.N. Ertas, *Synthesis, characterization and potent antibacterial activity of metal-substituted spinel ferrite nanoparticles.* Journal of Cluster Science, 2023. **34**(4): p. 2067-2078. DOI: 10.1007/s10876-022-02336-1
14. Haija, M.A., et al., *Adsorption and gas sensing properties of CuFe2O4 nanoparticles.* Mater. Sci. Pol, 2019. **37**: p. 289-295. DOI: 10.2478/msp-2019-0035
15. Erdawati, E. Allanas, and Y. Pratiwi. *Effectiveness biochar/CuFe2O4 as a media filter for water quality in the aquaponic system of gourami with bell pepper*. in *AIP Conference Proceedings*. 2021: AIP Publishing LLC. DOI: 10.1063/5.0052422

16. Mulud, F.H., N.A. Dahham, and I.F. Waheed. *Synthesis and characterization of copper ferrite nanoparticles*. in *IOP Conference Series: Materials Science and Engineering*. 2020: IOP Publishing. DOI: 10.1088/1757-899X/881/1/012084
17. Jimaa, R.B. and Z.H. Mahmoud, *Evaluation the Efficiency of $CuFe_2O_4$ Prepared Photolysis by OSD and Photo degradation.* Entomology and Applied Science Letters, 2018. **5**(2-2018): p. 91-100.
18. Satheeshkumar, M., et al., *Structural and magnetic properties of CuFe2O4 ferrite nanoparticles synthesized by cow urine assisted combustion method.* Journal of Magnetism and Magnetic Materials, 2019. **484**: p. 120-125. DOI: 10.1016/j.jmmm.2019.03.037
19. Atia, T.A., et al., *Synthesis and characterization of copper ferrite magnetic nanoparticles by hydrothermal route.* Chemical Engineering Transactions, 2016. **47**: p. 151-156. DOI: 10.3303/CET1647026
20. Liu, H., et al., *Effect of temperature on the size of biosynthesized silver nanoparticle: Deep insight into microscopic kinetics analysis.* Arabian Journal of Chemistry, 2020. **13**(1): p. 1011-1019 .DOI: 10.1016/j.arabjc.2019.11.011
21. Martínez-Montelongo, J.H., et al., *Antimicrobial activity of CuFe2O4 and CuFe2O4/ZnO: Squaring colorimetric and traditional microbiology assays with atomic force-and holotomography-microscopies.* Ceramics International, 2025. **51**(2): p. 2452-2466. DOI: 10.1016/j.ceramint.2024.08.279
22. Gu, Y., et al., *Bacterial disinfection by CuFe2O4 nanoparticles enhanced by NH2OH: A mechanistic study.* Nanomaterials, 2019. **10**(1): p. 18. DOI: 10.3390/nano10010018
23. Amini, M., et al., *Spinel copper ferrite nanoparticles: Preparation, characterization and catalytic activity.* Applied Organometallic Chemistry, 2018. **32**(9): p. e4470. DOI: 10.1002/aoc.4470

## تحضير وتشخيص ودراسة النشاط المضاد للبكتريا لجسيمات نانوية من أوكسيد الحديد النحاسي ($CuFe_2O_4$) وقياس سميتها

**ايمان مظهر إسماعيل [1]، مروه صلاح غفوري [2]، نور علي حسن [3]، عذراء محمد رشيد [4]**

**[1,2]مديرية تربية ديالى**
**[3,4] جامعة ديالى, كلية التربية للعلوم الصرفة, قسم الكيمياء**

**المستخلص**

لجسيمات النانوية المعدنية (NPs) تطبيقات هائلة بسبب خصائصها الفيزيائية والكيميائية الرائعة. لقد كان تخليق NPs مصدر قلق لأن الطرق الكيميائية سامة. تم تحضير مركبات الاسبينل النانوية CuFe2O4 باستخدام طريقة الكيمياء الخضراء وتم تشخيصها باستخدام تحويل فوريه للأشعة تحت الحمراء (FTIR)، على سبيل المثال، المجهر الإلكتروني الماسح (SEM)، التحليل الطيفي EDX، وحيود الأشعة السينية (XRD). أظهر التحليل الطيفي FTIR لـ CuFe2O4 نطاقين عريضين عند 365 و547 سم-1. أظهرت نتائج حيود الأشعة السينية أن متوسط حجم الجسيمات كان 30.62 نانومتر. أظهرت صور المجهر الإلكتروني الماسح (SEM) شكلاً قرصياً غير منتظم للجسيمات النانوية، والتي تتكتل بشكل أكبر في حالة التخليق الأخضر. وتُظهر صورة المجهر الإلكتروني الماسح لجسيمات CuFe2O4 النانوية شكلاً كروياً في الغالب. وتُظهر الجسيمات تكتلاً ملحوظاً، مما ينتج عنه قطر متوسط يبلغ حوالي 107.24 نانومتر. تتوافق هذه النتائج بشكل جيد مع الدراسات السابقة المتعلقة بسلوك هياكل الفريت الإسبينلي النانوية. دُرست فعالية تثبيط مركبات CuFe2O4 المُحضّرة على بكتيريا الإشريكية القولونية المعزولة من مياه نهر ديالى. وقيس تثبيط مركبات الإسبينلي النانوية باستخدام خمسة تراكيز متتالية (500، 600، 700، 800، 900، و1000) ميكروغرام/مل. أظهرت النتائج أن مركب CuFe2O4 يمتلك فعالية مثبطة لنمو بكتيريا الإشريكية القولونية، حيث بلغت أعلى نسبة تثبيط للنمو 63.2% عند تركيز 1000 ميكروغرام/مل. أما عند تركيز 500 ميكروغرام/مل، فكانت أدنى نسبة تثبيط للنمو 17.6%. دُرست سمية مركبات CuFe2O4 على خط خلايا HUVEC البطانية باستخدام اختبار MTT. بلغت نسبة بقاء خلايا HUVEC بعد 48 ساعة من إضافة فيريت النحاس (CuFe2O4) بتركيز 25 ميكروغرام/مل 99.70%، وهو أدنى تركيز، بينما بلغت نسبة بقاء خلايا HUVEC عند أعلى تركيز (400 ميكروغرام/مل) 45.38%، وكانت قيمة IC50 تساوي 311.